Struct Multidisc Optim (2014) 50:701–716
DOI 10.1007/s00158-014-1079-x

INDUSTRIAL APPLICATION

Seismic optimum design of triple friction pendulum bearing subjected to near-fault pulse-like ground motions

Hesamaldin Moeindarbari · Touraj Taghikhany

Received: 1 August 2013 / Revised: 18 February 2014 / Accepted: 28 February 2014 / Published online: 11 June 2014

Abstract Triple Friction Pendulum Bearing (TFPB) as a novel seismic isolator, provides different combinations of stiffness and damping during its course of motion. The adaptive behavior of TFPBs is one of the practical solutions for unsuitable performance of seismic isolation systems under near-fault ground motions. Selecting the TFPB's design variables (curvature radii, friction coefficients and displacement capacity of sliding surfaces) is complicated process while finding the optimized combination of these variables depends on input ground motion characteristics and seismic performance objectives of the superstructure. Here first, comprehensive nonlinear dynamic analyses are performed to identify influence of the design variables on superstructure response (roof acceleration and displacement of isolated level). Next, a specific numerical optimization method based on Genetic Algorithms (GA) is applied to determine the optimum values of the design variables that minimize superstructure demands. In this process, near-fault ground motions are employed with ranges of pulse periods and hazard levels as input excitations. According to GA results, the derived optimum design variables of TFPB have significantly distinct intervals for different target responses such as story drift and TFPB displacement. Therefore response targets (single objective functions) are combined to make a new fitness function. The proposed optimization method for determining design variables and design intervals can be used for investigating many other types of superstructures with similar behaviors.

Keywords Seismic isolation · Triple friction pendulum · Near-fault ground motion · Genetic algorithm · Optimization

H. Moeindarbari · T. Taghikhany (✉)
Department of Civil and Environmental Engineering, Amirkabir University of Technology, Tehran, Iran
e-mail: ttaghikhany@aut.ac.ir

H. Moeindarbari
e-mail: hessammoeen@aut.ac.ir

1 Introduction

After extensive damages observed in engineering designed structures due to vicinity of seismic sources (Bertero et al. 1978; Alavi and Krawinkler 2001; Yang et al. 2005), many researches have been conducted to study the nature of ground motion in close distances of causative faults (Hall et al. 1995). Indeed, there are varieties of characteristics for these kinds of ground motions that have encouraged engineers to find advance technologies to improve seismic resistance of structures against such kinds of vibrations. One of the applicable technologies is seismic isolation that has wide range of well-known applications and different construction methods. Among different types of implemented isolators, Friction Pendulum System (FPS), a first generation of friction concave isolators, is one of the famous systems that was invented by Zayas in 1986 (Zayas et al. 1990). It consists of a spherical concave sliding surface and a slider as an innovative bearing that exerts friction as supplemental damping. Because of the gravitational load of superstructure transmitted to the concave surface, FPS can provide a restoring force that reduces the residual displacement. The spherical concave surface inevitably produces a constant vibration period for the isolated structure depending on the curvature radius of the sliding surface. Nevertheless, under long periods of near-fault ground motions the efficiency of FPS is doubtful due to its large amplitudes of ground motion (Jangid

2005). This problem can be solved by adding supplemental dampers in isolation level. However supplemental dampers increase floor acceleration and damages of sensitive equipment even in low level earthquakes.

In this regard, multiple pendulums bearing such as Double and Triple Friction Pendulum Bearing (DFPB, TFPB) were invented in such a way to restrict the base displacement and floor acceleration simultaneously by applying variable stiffness and damping during their course of motion (Tsai et al. 2004). TFPB (Fig. 1a) enables engineers to choose a desirable combination of stiffness and damping in certain levels of excitation and to acquire multiple performance objectives that were not accessible by using traditional base isolation systems (Fenz and Constantinou 2008a, b, c; Malekzadeh and Taghikhany 2012).

Selecting an optimum set of the design variables in TFPB, such as radii of curvature, friction coefficients and displacement capacities of each concave surface, is an abstruse task since their optimum values depend on input ground motion characteristics and seismic performance objective of the superstructure.

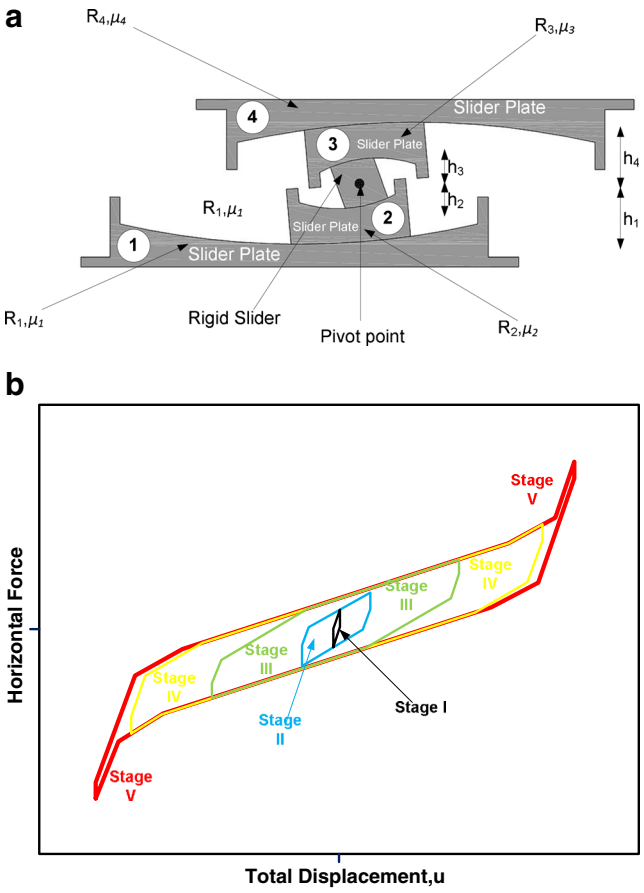

Fig. 1 **a** Section of a TFPB, **b** Different stages of sliding related to adaptive TFPB

Herein, after a precise numerical modeling of TFPB, sensitivity analysis was done to characterize effects of variation of design variables on seismic response of the superstructure. The variation of design variables was determined according to practical ranges for common buildings (not special structures like bridges). In next step, design variables and their combinations that can minimize superstructure demands (such as floor acceleration, drift ratio and base displacement) were obtained. In this procedure, near-fault strong ground motions with different characteristics in three hazard levels were used. During these procedures optimum design variables for nonlinear implicit target functions were acquired using Genetic Algorithm (GA) as an evolutionary population-based meta-heuristic method of optimization.

2 Adaptive triple friction pendulum bearings (TFPB)

Triple Friction Pendulum Bearing (Fig. 1a) consists of four stainless steel concave surfaces separated by an internal rigid slider. All four surfaces are coated with a non-metallic sliding material. As shown in Fig. 1a, R_i is the radius of curvature of the surface i, h_i is the radial distance between the pivot point and the surface i and μ_i is the coefficient of friction at the sliding interface. Throughout the course of motion, the internal construction of these bearings induce sliding to occur on different combinations of surfaces that results in changes of stiffness and damping (Fenz and Constantinou 2008c). Different stages of sliding that are related to adaptive TFPB during different levels of excitation are defined as follows (Fig. 1b):

Stage I Sliding is on surface 2 and 3. This stage forms only one pendulum mechanism and defines the properties of the isolation system under low levels of excitation (Service Level Earthquake: SLE).

Stage II Stopping of motion on surface 2 and then sliding on surfaces 1 and 3. This mechanism defines the primary properties of the isolation system under moderate levels of excitation (Design Basis Earthquake: DBE).

Stage III Stopping of motion on surfaces 2 and 3 and then sliding occur on surface 1 and 4.The friction coefficient of upper concave surface 4 is sufficiently large to prevent sliding until extreme levels of excitations (Maximum Credible Earthquake: MCE).

Stage IV Contacting of slider to the restrainer on surface 1. Motion remains stopped on surface 3 and sliding occurs on surfaces 2 and 4. This mechanism

defines properties of isolation bearing beyond MCE.

Stage V Bearing of slider on restrainer of surfaces 1 and 4 and then sliding continues on surfaces 2 and 3.

The behavior of Triple Friction Pendulum Bearing is termed "adaptive" if it progressively exhibits various hysteretic properties at all of stages shown in Fig. 1b. The stiffness and damping can be changed to predictable values at different controllable amplitudes. These properties let the design of isolation system to be separately optimized in multiple levels of input excitation. As it is shown in Fig. 2 the hysteretic behavior of TFPBs is simulated by series model consists of three independent single friction pendulum bearings (SFPBs) according to the work reported by Fenz and Constantinou (2008b). Each independent single friction pendulum bearing in this model consists of three parallel elements:

a) Linear elastic spring that creates the resistance force in concave surfaces
b) Velocity dependent friction element with rigid plastic nonlinear behavior
c) Gap element that accounts for the finite displacement capacity of each sliding surface.

Each linear elastic spring has the stiffness of $\frac{1}{\overline{R}_{effi}}$ where $\overline{R}_{effi}$ is the effective radius of curvature $(R_i - h_i)$ and for each gap element $\overline{d}_i$ is the displacement capacity. In rigid plastic friction elements the velocity dependent coefficient of friction for each element is $\overline{\propto}_i$. The dependency of coefficient of friction to the velocity is given by the following equation (Constantinou et al. 1990; Mokha et al. 1990):

$$\mu = f_{\max} - (f_{\max} - f_{\min}) \exp(-a\,|\dot{u}|)\,, \tag{1}$$

Where f_{max} is the friction coefficient due to high velocities, f_{min} is the friction coefficient in lowest (or negligible) velocities and *a is* the rate parameter that adjusts the rate of the transition of friction coefficient between f_{max} and f_{min}.

To obtain tri-linear adaptive behavior of TFPB (Fig. 1b), the characteristics of three elements in each SFPB ($\overline{R}_{effi}$,$\overline{\propto}_i$ and $\overline{d}_i$) should be selected according to Table 1. Considering other values for these parameters that are not consistent with the formulations presented in Table 1 generates disapproval hysteretic behavior for TFPB with no advantage to other sliding isolators.

3 Numerical modeling and verification

Figure 3 shows a schematic of a one story superstructure that is used for numerical modeling of TFPB in this study. As shown, the superstructure is assumed to be one degree of freedom model. The researches on behavior of short and medium stories isolated buildings with low damping bearings have been demonstrated that the effect of dynamic characteristics of superstructure on seismic performance of isolated systems is negligible (Kelly and Naeim 1999). The only cases which dynamic characteristics of superstructure influence on seismic isolation behavior are tall buildings or structures using highly damped bearings. In both cases, the purpose of application of seismic isolation is dissipating energy than period elongation. To optimize TFPB in common application of isolation systems (medium stories isolated buildings with medium damping), one degree of freedom model acceptably

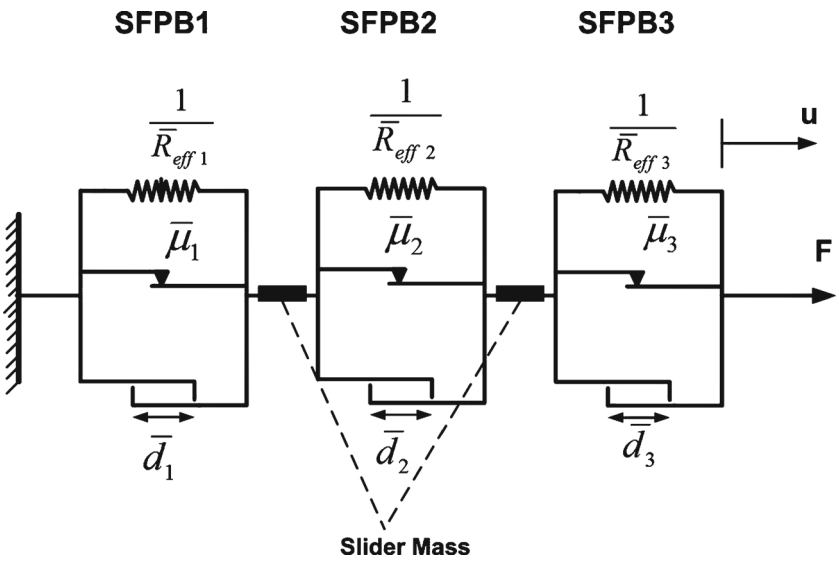

Fig. 2 Three SFPB connected in series to model a TFPB

Table 1 The variables of series model in terms of TFPB variables in a fully adaptive arrangement (Fenz and Constantinou 2008b)

	Coefficient of friction	Radius of curvature	Nominal displacement capacity	Rate parameter
Element 1	$\overline{\propto}_1 = \propto_2 = \propto_3$	$\overline{R}_{eff1} = R_{eff2} + R_{eff3}$	$\overline{d}_1 = d_{tot} - (\overline{d}_2 + \overline{d}_3)$	$\overline{a}_1 = \frac{1}{2}\frac{a_2+a_3}{2}$
Element 2	$\overline{\propto}_2 = \propto_1$	$\overline{R}_{eff2} = R_{eff1} - R_{eff2}$	$\overline{d}_2 = \frac{R_{eff1}-R_{eff2}}{R_{eff1}} d_1$	$\overline{a}_2 = \frac{R_{eff1}}{R_{eff1}-R_{eff2}} a_1$
Element 3	$\overline{\propto}_3 = \propto_4$	$\overline{R}_{eff3} = R_{eff4} + R_{eff3}$	$\overline{d}_3 = \frac{R_{eff4}-R_{eff3}}{R_{eff4}} d_4$	$\overline{a}_3 = \frac{R_{eff4}}{R_{eff4}-R_{eff3}} a_4$

anticipates dynamic behavior of this systems and dominates higher modes of vibration in multi degree of freedom models. The differential equations of motion are used to predict motion of four masses of the isolated system in figure. In each SFPB element of series model the transmitting force is calculated by:

$$F_i = \frac{W}{N_{TFPB} R_{effi}} u_i + \mu_i \frac{W}{N_{TFPB}} z_i + \underbrace{k_{ri} \left(|u_i| - d_i\right) sgn\left(u_i\right) H\left(|u_i| - d_i\right)}_{F_{ri}} \tag{2}$$

Where W is weight of structure and N_{TFPB} is number of TFPBs used in isolation system. The relative displacement for each element is u_i and Z_i is the hysteretic variable that varies between 1 and -1 governed by (3). k_{ri} is the stiffness exhibited by the displacement restrainers in the i^{th} element and d_i is the displacement capacity of each gap element. In this equation H is a Heaviside step function. The hysteretic variable Z_i is governed by following differential equation (Fenz 2008):

$$\frac{dZ_i}{dt} = \frac{1}{u_{yi}} \left\{A_i - |Z_i|^{\eta_i} \left[\gamma_i sign(\dot{u}_i Z_i) + \beta_i\right]\right\} \dot{u}_i \tag{3}$$

Where $\dot{u}_i$ is the sliding velocity in each element and u_{yi} is yield displacement parameter. γ_i, η_i, β_i, A_i are dimensionless parameters that control the shape of hysteretic loop. Here consistent with Fenz et al (Fenz and Constantinou 2008b), the following values are assumed for these parameters: $u_{yi} = 0.01$, $A_i = 1$, $\gamma_i = 0.9$ and $\eta_i = \beta_i = 2$. In a one story superstructure supported by TFPB system as shown in Fig. 3, the equations of motion are used to predict motion of four different masses. The equations of motion for an isolated system with four degrees of freedom (as shown in Fig. 3) are obtained:

$$m_4 \ddot{u}_4 + c_s(\dot{u}_4 - \dot{u}_3) - k_s(u_4 - u_3) = -m_4 \ddot{u}_g(t) \tag{4}$$

$$m_3 \ddot{u}_3 + N_{TFPB}\left[\frac{W}{N_{TFPB} R_{eff3}}(u_3 - u_2) + \mu_3 \frac{W}{N_{TFPB}} Z_3 + k_{r3}(|u_3 - u_2| - d_3) sgn(u_3 - u_2) H(|u_3 - u_2| - d_3) - \frac{C_s}{N_{TFPB}}(\dot{u}_4 - \dot{u}_3) - \frac{K_s}{N_{TFPB}}(u_4 - u_3)\right] + C_b \dot{u}_3 = -m_3 \ddot{u}_g(t) \tag{5}$$

$$m_2 \ddot{u}_2 + \frac{W}{N_{TFPB} R_{eff2}}(u_2 - u_1) + \mu_2 \frac{W}{N_{TFPB}} Z_2 + F_{r2} - \frac{W}{N_{TFPB} R_{eff3}}(u_3 - u_2) - \mu_3 \frac{W}{N_{TFPB}} Z_3 - F_{r3} = -m_2 \ddot{u}_g(t) \tag{6}$$

$$m_1 \ddot{u}_1 + \frac{W}{N_{TFPB} R_{eff1}} u_1 + \mu_1 \frac{W}{N_{TFPB}} Z_1 + F_{r1} - \frac{W}{N_{TFPB} R_{eff2}}(u_2 - u_1) - \mu_2 \frac{W}{N_{TFPB}} Z_2 - F_{r2} = -m_1 \ddot{u}_g(t) \tag{7}$$

Where the hysteretic variables Z_i in above equations are derived using following relationships:

$$\frac{dZ_1}{dt} = \underbrace{\frac{1}{u_{y1}} \left\{A_1 - |Z_1|^{\eta_1} \left[\gamma_1 sgn(\dot{u}_1 Z_1) + \beta_1\right]\right\} \dot{u}_1}_{z_1} \tag{8}$$

$$\frac{dZ_2}{dt} = \underbrace{\frac{1}{u_{y2}} \left\{A_2 - |Z_2|^{\eta_2} \left[\gamma_2 sgn((\dot{u}_2 - \dot{u}_1) Z_2) + \beta_2\right]\right\}}_{z_2} (\dot{u}_2 - \dot{u}_1) \tag{9}$$

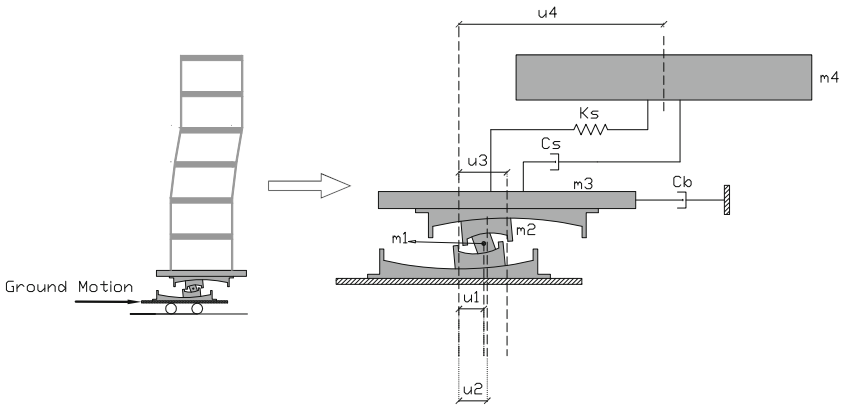

Fig. 3 Schematic of SDOF system isolated with TFPB

$$\frac{dZ_3}{dt} = \underbrace{\frac{1}{u_{y3}}\left\{A_3 - |Z_3|^{\eta_3}\left[\gamma_3 sgn((\dot{u}_3 - \dot{u}_2)Z_3) + \beta_3\right]\right\}}_{z_3}(\dot{u}_3 - \dot{u}_2) \tag{10}$$

As shown in Fig. 3, m_i is the mass of i^{th} slider ($i = 1, 2, 3$) and m_4 the mass of superstructure. Matrix notation is employed as an alternative way of presenting above first order ordinary differential equations of motion:

$$\{\dot{X}\} = [A]\{X\} + \{B\} \tag{11}$$

Where the state vector {x} is:

$$\{\mathrm{x}\} = \{\mathrm{u}_1\ \mathrm{u}_2\ \mathrm{u}_3\ \mathrm{u}_4\ \dot{\mathrm{u}}_1\ \dot{\mathrm{u}}_2\ \dot{\mathrm{u}}_3\ \dot{\mathrm{u}}_4\ \mathrm{Z}_1\ \mathrm{Z}_2\ \mathrm{Z}_3\}^{\mathrm{T}} \tag{12}$$

And matrix A and B are expresses as:

$$A = \begin{bmatrix}
0 & 0 & 0 & 0 & 1 & 0 & 0 & 0 & 0 & 0 & 0 \\
0 & 0 & 0 & 0 & 0 & 1 & 0 & 0 & 0 & 0 & 0 \\
0 & 0 & 0 & 0 & 0 & 0 & 1 & 0 & 0 & 0 & 0 \\
0 & 0 & 0 & 0 & 0 & 0 & 0 & 1 & 0 & 0 & 0 \\
\frac{W}{N_{TFPB}m_1R_{eff1}} + \frac{W}{N_{TFPB}m_1R_{eff2}} & \frac{W}{N_{TFPB}m_1R_{eff2}} & 0 & 0 & 0 & 0 & 0 & 0 & \mu_1\frac{W}{N_{TFPB}m_1} & \mu_2\frac{W}{N_{TFPB}m_1} & 0 \\
\frac{W}{N_{TFPB}m_2R_{eff2}} & -\left[\frac{W}{N_{TFPB}m_2R_{eff2}} + \frac{W}{N_{TFPB}m_2R_{eff3}}\right] & \frac{W}{N_{TFPB}m_2R_{eff3}} & 0 & 0 & 0 & 0 & 0 & 0 & -\mu_2\frac{W}{N_{TFPB}m_2} & \mu_3\frac{W}{N_{TFPB}m_2} \\
0 & \frac{W}{m_3R_{eff3}} & -\left[\frac{W}{m_3R_{eff3}} + \frac{k_s}{m_3}\right] & \frac{k_s}{m_3} & 0 & 0 & \frac{-(c_s+c_b)}{m_3} & \frac{c_s}{m_3} & 0 & 0 & -\mu_3\frac{W}{m_3} \\
0 & 0 & \frac{k_s}{m_4} & \frac{k_s}{m_4} & 0 & 0 & \frac{c_s}{m_4} & -\frac{c_s}{m_4} & 0 & 0 & 0 \\
0 & 0 & 0 & 0 & z_1 & 0 & 0 & 0 & 0 & 0 & 0 \\
0 & 0 & 0 & 0 & -z_2 & z_2 & 0 & 0 & 0 & 0 & 0 \\
0 & 0 & 0 & 0 & 0 & -z_3 & z_3 & 0 & 0 & 0 & 0
\end{bmatrix}$$

$$B = \left[0;\ 0;\ 0;\ 0;\ \frac{F_{r2}}{m_1} - \frac{F_{r1}}{m_1} - \ddot{u}_g(t);\ -\frac{F_{r2}}{m_2} + \frac{F_{r3}}{m_2} - \ddot{u}_g(t);\ \frac{F_{r3}}{m_3} - \ddot{u}_g(t);\ -\ddot{u}_g(t);\ 0;\ 0;\ 0;\right]^T$$

A code with MATLAB language was used to obtain solutions of equations and the results were verified and compared with numerical outcomes reported by Fenz and Constantinou (2008b). The specifications of the one story superstructure in experimental model are shown in Fig. 4. For the verification the 180 degree component of the 1940 El Centro record with the PGA = 0.31 g was used in time history nonlinear analysis. To induce isolator displacement such that having all the sliding regimes in the TFPB's behavior, the record was multiplied by a factor of 2.15. The variables of TFPB and its equal series model that was used in our verification model are presented in Table 2 in compliance with limitations shown in Table 1. In this study "ode15" a built-in MATLAB function is applied to solve the state equation.

Figures 5 and 6 show force-displacement diagrams of TFPB and acceleration time history of roof respectively. In these figures our results from numerical modeling are compared with the outcomes reported by Fenz and Constantinou (2008b). It is concluded that our results within a tolerable error can be used to predict real responses of superstructure and isolator.

4 Input ground motions

Doubtful behavior of traditional seismic isolators under large absolute amplitude of velocity pulse and long period of near-fault ground motions was the main reason to study how to choose combination of stiffness and damping in TFPB to acquire appropriate behavior. Due to complex hysteretic behavior of TFPB and role of design variables in this behavior, time history analysis should be applied in optimization procedure. Accordingly, selecting the ground motions for this study that represents broad range of amplitude and pulse period of near-fault ground motion is crucial. Table 3 shows a list of pulse-like near-fault ground motions selected in this study. In this Table, seven records with pulse periods between 1 and 7 seconds have been adopted to cover a wide range of pulse periods in near-fault ground motions. These ground motions were selected from PEER-NGA database according to Baker's studies in 2007 (Baker 2007).

To have a right judgment regarding the sensitivity analysis and to observe all stages of nonlinear behavior of adaptive TFPBs, input accelerograms have been normalized to three levels of MCE, DBE and SLE. The design peak ground acceleration for these levels were considered to be 0.759, 0.517 and 0.291 of gravity acceleration respectively according to PSHA analysis for a case study region in Iran (Qazvin City). In spite of the fact that these particular hazard levels limits the generality of the obtained results for optimum parameters, each level is not so different comparing with hazard levels in other parts across the world. The derived results support the decency of this assumption as well.

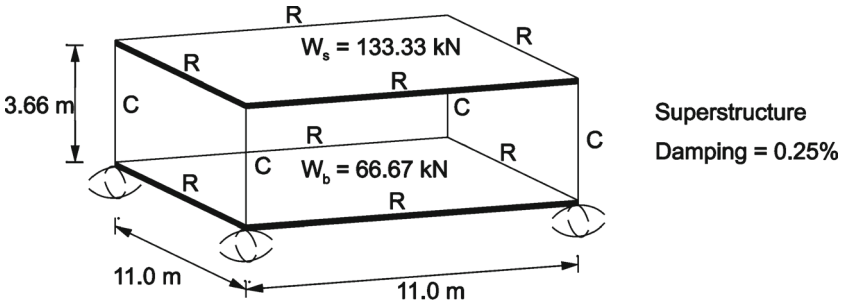

Fig. 4 The specification of isolated superstructure used for verification of model(Fenz and Constantinou 2008b)

Section Property	Area (mm^2)	Moments of Inertia (mm^4)	Torsion Constant (mm^4)	Shear Area (mm^2)	Mass (kg)	Weight (kN)
"Column" (C)	5.0×10^6	6.851×10^7	1.0×10^8	5.0×10^6	0	0
"Rigid" (R)	5.0×10^6	1.0×10^{11}	1.0×10^8	5.0×10^6	0	0

5 Sensitivity analysis

Sensitivity analysis is employed to determine how variations of independent design variables impact dependent responses under strong seismic motions. This technique is used within specific boundaries for each design variable according to practical ranges available for buildings and current products. Sensitivity analysis is a way to decide about selecting those design variables that have the key role in optimum design of TFPB. This technique can determine how changes in design variables of TFPB will impact the target variables such as base displacement or roof acceleration of isolated structures. Here for sensitivity analysis seven independent design variables of TFPB were selected to observe the response of structure under seven pulse-like ground motions in three earthquake design levels (MCE, DBE and SLE). The chosen variables are:

Variable No 1: Effective radius of curvature of sliding surfaces 1 and 4, R_{eff1}

Variable No 2: Effective radius of curvature of sliding surfaces 2 and 3, R_{eff2}

Variable No 3: Coefficient of friction of sliding surface 1, μ_1

Variable No 4: Coefficient of friction of sliding surfaces 2 and 3, μ_2

Variable No 5: Coefficient of friction of sliding surface 4, μ_4

Variable No 6: Displacement capacity of sliding surfaces 1 and 4, d_1

Variable No 7: Displacement capacity of sliding surfaces 2 and 3, d_2

There are several variables that could control the response of TFPB or superstructure, however these can

Table 2 The properties of TFPB and alternative series elements(Fenz and Constantinou 2008b)

Properties of TFPB				
Surface 1	$R_{eff1} = 435$ mm	$\mu_1 = 0.02-.04$	$d_1 = 54$ mm	$a_1 = 0.1$ sec/mm
Surface 2	$R_{eff2} = 53$ mm	$\mu_2 = 0.01-0.02$	$d_2 = 19$ mm	$a_1 = 0.1$ sec/mm
Surface 3	$R_{eff3} = 53$ mm	$\mu_3 = 0.01-0.02$	$d_3 = 19$ mm	$a_1 = 0.1$ sec/mm
Surface 4	$R_{eff4} = 435$ mm	$\mu_4 = 0.06-0.13$	$d_4 = 64$ mm	$a_1 = 0.1$ sec
Properties of series elements				
Element 1	$\overline{R}_{eff1} = 106$ mm	$\overline{\mu}_1 = 0.01 - 0.02$	$\overline{d}_1 = 53.6$ mm	$\overline{a}_1 = 0.05$ sec/mm
Element 1	$\overline{R}_{eff2} = 382$ mm	$\overline{\mu}_2 = 0.02 - 0.04$	$\overline{d}_2 = 56.2$ mm	$\overline{a}_2 = 0.05$ sec/mm
Element 1	$\overline{R}_{eff3} = 382$ mm	$\overline{\mu}_3 = 0.06 - 0.13$	$\overline{d}_3 = 56.2$ mm	$\overline{a}_3 = 0.05$ sec/mm

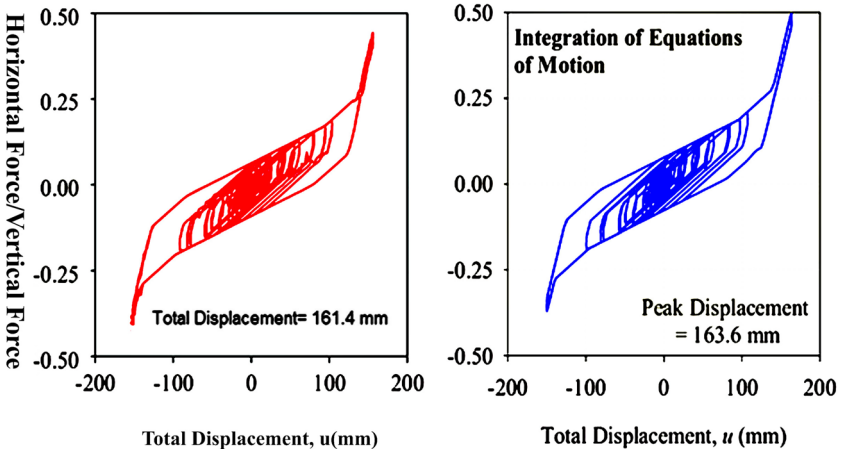

Fig. 5 TFPB force-displacement: Comparison of our results (*left*) with the results reported by Fenz and Constantinou(Fenz and Constantinou 2008b) (*right*)

be limited to seven variables considering following assumptions:

- The isolator is considered as "fully adaptive". This term is used (Fenz and Constantinou 2008a) for isolators which their specifications (such as coefficients of friction and radii of curvature) are chosen in an arrangement such that all sliding stages can occur in different levels of excitation. According to this assumption, sliding surfaces 1 and 4 have equal radius of curvature as well as sliding surfaces 2 and 3. Furthermore, the coefficient of friction for sliding surfaces 2 and 3 are also considered to be equal for adaptive TFPB.
- Due to practical limitations, displacement capacity (d_i) of sliding surfaces 1 and 2 are considered to be equal and also coefficient of friction for sliding surface 4 is assumed to be the same as surface 3.
- Rate parameter "a" for all sliding surfaces is assumed to be 0.1 sec/mm that is a reasonable value.
- Considering previously reported values and also to limit the number of effective design variables, the upper bound of coefficient of friction f_{max} is considered twice larger than the lower bound f_{min}. So only f_{min} is considered as the independent variable.
- The stiffness of restrainers, k_r is considered to be a large value (17,500kN/mm for all sliding surfaces).

In sensitivity analysis, one of the variables is considered to be changed in a specific range while other design variables stay constant. The variation interval

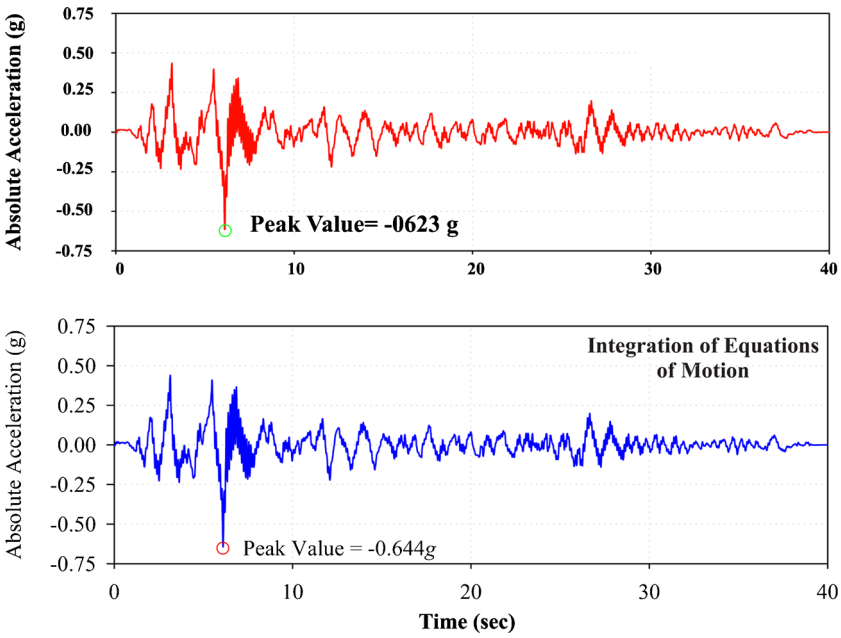

Fig. 6 Absolute acceleration of the superstructure roof: Comparison of our results with the results reported by Fenz and Constantinou (Fenz and Constantinou 2008b)

Table 3 Specifications of Input ground motions

Record No.	Name of earthquake	Year	Record No. in baker classification	Station	Pulse period T_p(sec)	Magnitude (M_w)
1	Morgan Hill	1984	24	Coyote Lake Dam (SW Abut)	1	6.2
2	Loma Prieta	1989	33	Alameda Naval Air Stn Hanger	2	6.9
3	Cape Mendocino	1992	38	Petrolia	3	7
4	Imperial Valley-06	1979	13	EI Centro Array #6	3.8	6.5
5	Imperial Valley-06	1979	14	EI Centro Array #7	4.2	6.5
6	Landers	1992	40	Lucerne	5.1	7.3
7	Chi-Chi, Taiwan	1999	64	TCU038	7	7.6

and constant values for seven selected design variable are shown in Table 4. The interval for each variable is specified according to values suggested by manufacturers and also latest researches and tests (Fenz and Constantinou 2008a; Moeindarbari et al. 2014). It is clear that the optimum parameters are significantly limited by the choice of ranges for bearing dimensions. However, since the purpose of this study is optimizing the parameters of TFPB in its common application for medium stories isolated buildings (btw 8 and 12 stories), having an isolation system with maximum effective period between 2 and 3 seconds will be reasonable (Mayes and Naeim 2001). The maximum curvature radius of 1 meter for TFPB will produce a vibration period of about 2.8 seconds that seems to be acceptable for this study.

It is also important to mention that the coefficients of friction is defined as a proposed range of values of the coefficients for normal temperature and without any effects for aging, contamination and history of loading, and are for a fresh bearing at normal temperature.

The constant values are chosen equal to the values used for verification model described in Section 3.

Table 4 The values of design variables for sensitivity analysis

	Variation interval of each parameter	Constant value of each parameter
R_{eff1}(m)	0.44 – 1	0.435
R_{eff2}(m)	0.044 – 0.1	0.053
μ_1	0.018 – 0.06	0.02
μ_2	0.01 – 0.02	0.015
μ_3	0.05 – 0.15	0.06
d_1(m)	0.054 – 0.11	0.064
d_2(m)	0.022 – 0.05	0.019

6 Results of sensitivity analysis

6.1 Maximum relative story displacement (MRSD)

Maximum Relative Story Displacement (MRSD) is considered as one of the commonly used seismic demands for evaluation of seismic performance of structures. Accordingly investigating the influence of variation of TFPB design variables on MRSD of superstructure provides a general prospect of seismic performance of an isolated structure. Figure 7 shows maximum relative story displacement of superstructure (MRSD) under ground motion record No.1 versus variation of effective radius of curvature of sliding surfaces 1 and 4 (R_{eff1}) while other design variables of TFPB are constant. In this figure MRSD is normalized to its maximum value and its fluctuation has been plotted for three hazard levels. As it is shown in this figure the variation of normalized MRSD exhibits different trends for three hazard levels which indicates different behavior of TFPB under different levels of excitation. To summarize the sensitivity of TFPB under seven ground motions, the relative value of MRSD to its mean value in has been defined by "γ":

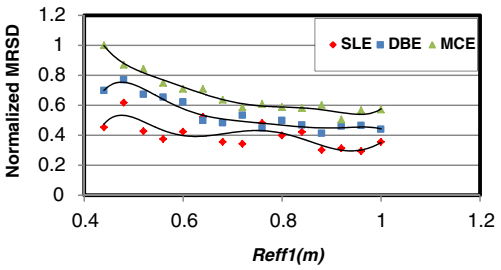

Fig. 7 Sensitivity of MRSD due to variation of R_{eff1} for ground motion number 1 in 3 hazard levels

$$\gamma = \frac{Max_R - Min_R}{\left(\frac{Max_R + Min_R}{2}\right)} \tag{13}$$

where Max_R and Min_R are the maximum and the minimum of MRSD during variation of R_{eff1} under specific ground motion respectively. For exampleMax_R, Min_R and γ for record 1 in MCE level are 1, 0.6 and 0.5 respectively (See Fig. 7). The maximum and minimum values of γ for seven records in three hazard levels are summarized in Table 5. According to Table 5 R_{eff1} can change the MRSD about 60 to 70 % of its mean value which clearly demonstrates the importance of R_{eff1} on MRSD. This result indicates that for optimum design of TFPB, R_{eff1} should be considered as a controlling variable.

6.2 Maximum horizontal floor acceleration (MHFA)

Maximum Horizontal Floor Acceleration (MHFA) is widely used by engineers to estimate the vulnerability of sensitive nonstructural elements or equipment. Since one of the main applications of seismic isolation is protecting nonstructural components in structures, it is necessary to investigate sensitivity of MHFA due to variation of TFPB variables. In this study, the superstructure assumed to be a single degree of freedom structure. So regarding to the fact that the rigid mode is the predominant vibration mode of isolated superstructures, the floor acceleration is a linear function of relative story displacement of superstructure. This can be perceived from Fig. 8 that compares the sensitivity of MRSD and the MHFA for Record No. 5. Therefore, MHFA is not considered as an independent object function and the effect of design variables on MHFA was not considered in sensitivity analysis and optimization process.

6.3 Maximum displacement in isolation level (MDIL)

In seismic isolated structures Maximum Displacement in Isolation Level (MDIL) is a decisive criterion which controls the size of surrounding trench of building. Consequently the effect of variation of TFPB design variables on MDIL is important. Figure 9 shows the sensitivity of MDIL under ground motion record No.6 for three hazard levels,

Table 5 Minimum and Maximum of γ for variable R_{eff1} according to MRSD variation

Hazard levels	MCE	DBE	SLE
Minimum ofγ (Percent)	8.9	9	27.1
Maximum of γ (Percent)	65.9	64.9	75

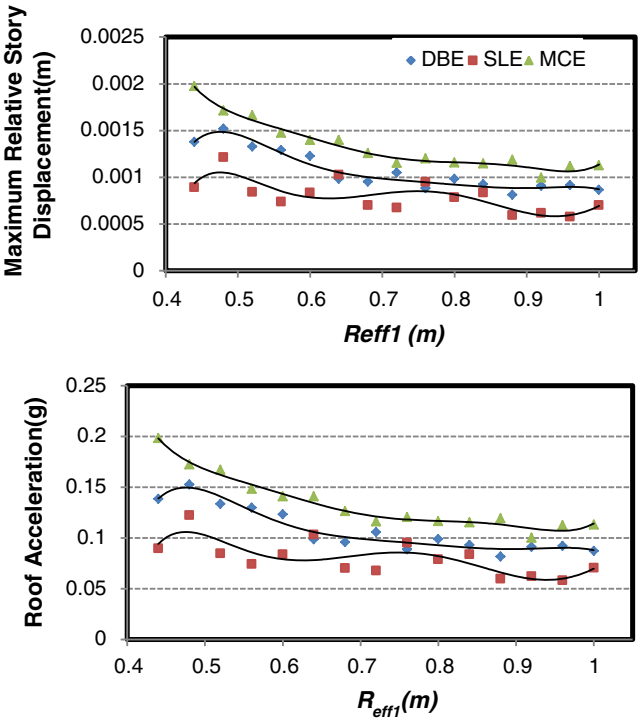

Fig. 8 Comparison of sensitivity of MRSD (upper graph) and MHFA (lower graph) to variation of R_{eff1} due to ground motion number 5 in three levels of hazard

when R_{eff1} varies and other design variables of TFPB are constant. As shown in this figure increasing R_{eff1} results in growing of MIDL. The maximum and minimum levels of γ for seven different records are presented in Table 6. According to these results and comparing them with Table 5, variation of R_{eff1} has lower influence on MDIL compared to MRSD.

6.4 Summary of the results of sensitivity analysis

The sensitivity analysis for other six design variables (R_{eff2}, μ_1, μ_2, μ_4, d_1, d_2) is summarized in Table 7. In this table the sensitivity of MRSD and MDIL due to the variation of design variables are shown using parameter γ. It can

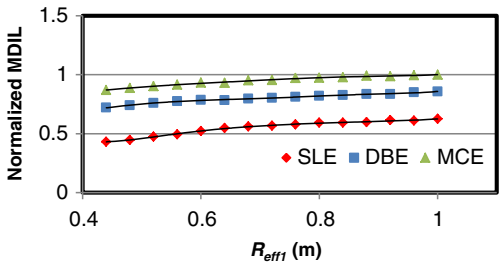

Fig. 9 Sensitivity of MDIL due to R_{eff1} variation for ground motion no.6 in three hazard levels

Table 6 Minimum and Maximum of γ for variable R_{eff1} according to MDIL variation

Hazard levels	MCE	DBE	SLE
Minimum of γ (Percent)	1	1.6	16.4
Maximum of γ (Percent)	24.5	31.8	37.1

be concluded that all variables have inevitable effect on the response of the structure. For R_{eff2} the largest value of γ is produced in MCE level. Varying R_{eff2}, γ fluctuates between 4.1 and 36.1 % for MRSD and 0.8 to 16.7 % for MDIL in 3 levels of hazard. It is clear that μ_1 plays an important role in controlling the value of MRSD and MDIL. For μ_1, MRSD has the largest value of $\gamma = 52.9$ % in DBE level and the smallest value of $\gamma = 3.1$ % in MCE level. μ_1 also affects the variation of MDIL significantly but not like MRSD. MDIL and MRSD exhibit lower sensitivity to μ_2 compared to μ_1 but effect of μ_2 is not negligible. μ_4 has the largest influence on variation of response of structure on MRSD in SLE level by having a $\gamma = 45.2$ %.

Comparing the effect of displacement capacities of sliding surfaces on response of structure, d_1 exhibits larger values of γ than d_2. For MRSD, γ has a large value of 104.4 % in DBE level due to the variation of d_1.

Table 7 Summary of sensitivity analysis for design variables

	Hazard level	MCE	DBE	SLE
Effective radius of curvature of sliding surfaces 2 and 3, $\boldsymbol{R_{eff2}}$				
MRSD	Minimum of γ (Percent)	4.8	4.1	5.7
	Maximum of γ (Percent)	3 6.1	25.2	31.8
MDIL	Minimum of γ (Percent)	0.8	1.8	2.4
	Maximum of γ (Percent)	16.7	7.3	8.1
Coefficient of friction of sliding surface 1, μ_1				
MRSD	Minimum of γ (Percent)	3.1	4.2	13.7
	Maximum of γ (Percent)	42.6	52.9	33.7
MDIL	Minimum of γ (Percent)	2.2	1.5	6.1
	Maximum of γ (Percent)	19.9	26.8	44.6
Coefficient of friction of sliding surface 2 and 3, μ_2				
MRSD	Minimum of γ (Percent)	1.9	3.6	9.1
	Maximum of γ (Percent)	26.1	21.5	42.3
MDIL	Minimum of γ (Percent)	0.3	1.1	4.2
	Maximum of γ (Percent)	11.3	2	1.2
Coefficient of friction of sliding surface 4, μ_4				
MRSD	Minimum of γ (Percent)	3.3	7.4	8.6
	Maximum of γ (Percent)	24.8	44.2	45.2
MDIL	Minimum of γ (Percent)	2.1	2.7	2.7
	Maximum of γ (Percent)	9.5	14.8	27.3
Displacement capacity of sliding surface 1 and 4, d_1				
MRSD	Minimum of γ (Percent)	9.4	0	0
	Maximum of γ (Percent)	71.6	104.4	82.7
MDIL	Minimum of γ (Percent)	2.1	0	0
	Maximum of γ (Percent)	57.8	35.2	24.2
Displacement capacity of sliding surface 2 and 3, d_2				
MRSD	Minimum of γ (Percent)	0	0	0
	Maximum of γ (Percent)	32.3	25.1	0
MDIL	Minimum of γ (Percent)	0	0	0
	Maximum of γ (Percent)	13.4	5.8	0

Table 8 Parameters of GA for optimizing process under 7 near-fault earthquake records

Record No.	Crossover fraction	Population size	Elite count
1	0.85	30	2
2	0.90	28	3
3	0.95	32	3
4	0.85	25	3
5	0.95	35	4
6	0.90	25	3
7	0.90	30	3

7 Optimum analysis of TFPB using genetic algorithm (GA)

Genetic Algorithm (GA) is a search meta-heuristic optimization tool that mimics the process of natural evolution. It is based on the idea that the productions of natural processes are optimum and also the method of reproduction in natural evolution is optimum itself. In GA a collection of feasible solutions (population or candidate solutions) is considered and then better solutions are respectively chosen using the sampling methods. The chosen chromosomes (solutions) are not always the chromosomes with best fitness function. Applying the same processes that governs the natural systems like mutation and crossover (recombination) on the chosen answers, in next step new collection of solutions will be generated as a new generation. These steps are iterated to reach more progressed generations with best mean fitness. At the end, the best chromosome of the generations with maximum fitness to the problem will be chosen as the optimum solution (Michalewicz 1995; Goldberg 1989).

The purpose of this research is to find the optimum design variables of TFPBs for near-fault ground motions. This is an optimization problem for minimizing specific implicit functions of design variables of a TFPB. Hence in this section, target response functions of design variables are defined as fitness functions for the GA optimization. The assumptions that are considered for GA optimization analysis are first described in the following section. Afterwards, the results of optimization process using GA for three levels of hazard are summarized using diagrams.

7.1 Defining problem and assumptions

In short and medium height isolated structures, the dynamic response of system is not hugely influenced by the superstructure specifications. The most effective parameter of superstructures that directly influence on the vibration period of first mode is total floor masses. But as it is known, the only property of pendulum bearings which dominates the vibration period of the first mode is radius of sliding surface. This trait makes the friction concave bearings different from the other types of isolation systems such as elastomeric ones where the vibration period of the structure is function of *total mass* of superstructure and *stiffness* of isolation system. Accordingly, the derived results from optimum solution analysis of TFPB have minimum dependence on superstructure characteristics and therefore it can be generalized for short and medium height isolated structures. Herein the overall specifications are two different structural demands: Maximum Relative Story Displacement (MRSD) and Maximum Displacement in Isolation Level (MDIL). In the first step of GA analysis fitness functions f_1 and f_2 are constructed as implicit function of TFPB seven design variables.

$$f_1\left(R_{eff1}, R_{eff2}, \mu_1, \mu_2, \mu_3, d_1, d_2\right) = (StoryDrift)_{max} = MRSD \tag{14}$$

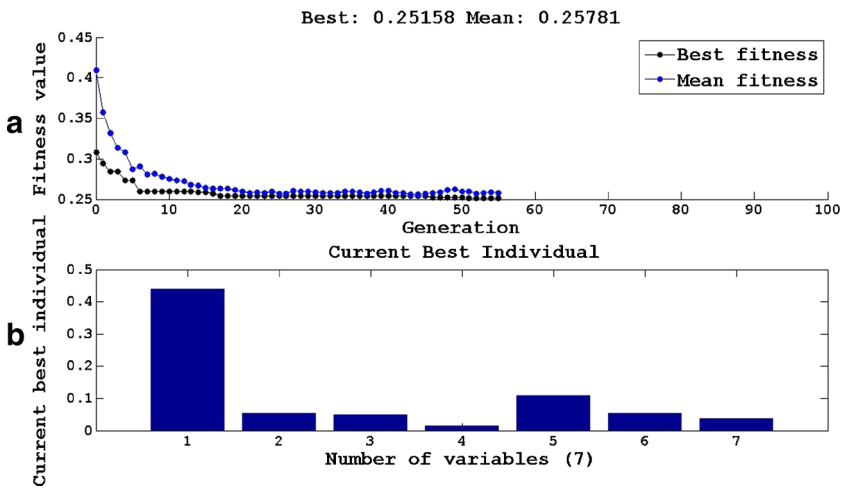

Fig. 10 **a** Convergence of mean and best values of f_2 after several generations during GA for implicit no.4 **b** optimum values of 7 design variables of TFPB

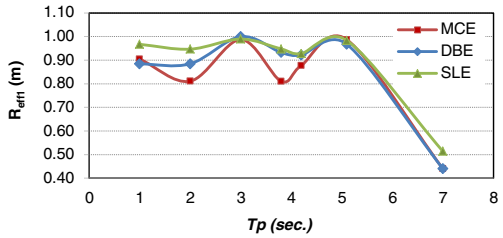

Fig. 11 Optimum values of R_{eff1} that minimize MRSD in three ground motion levels of MCE, DBE and SLE

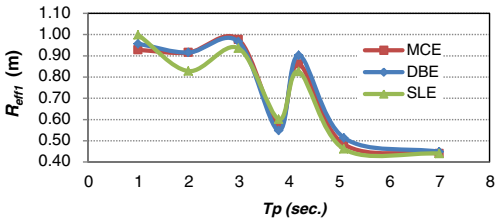

Fig. 13 The optimum values of R_{eff1} for combined objective function f in three levels of MCE, DBE and SLE

$$f_2\left(R_{eff1}, R_{eff2}, \mu_1, \mu_2, \mu_3, d_1, d_2\right) = (Isolator\,Level\,Displ.)_{max} = MDIL \tag{15}$$

Afterwards to simultaneously minimize both fitness functions f_1 (MRSD) and f_2 (MDIL) a new function is defined according to (16).

$$f\left(R_{eff1}, R_{eff2}, \mu_1, \mu_2, \mu_3, d_1, d_2\right) = \sum_{i=1}^{n} a_i \frac{f_i}{\min(f_i)} \tag{16}$$

Where n is the number of single objective functions (Here n = 2)*and* a_i is the weight of each single objective functions and is considered to be equal so $a_1 = a_2 = \frac{1}{n} = 0.5$. Hence function f is a summation of single objective functions, it is known as a Combined Objective function.

To satisfy the "fully adaptive" assumption consistent with Table 1 and to consider modeling assumptions, a nonlinear constraint function was used together with described interval limitations. The population type of GA was considered as a real vector and its size was initially chosen to be 20. The "creation function" which is responsible for creating new chromosomes (solutions) was considered as a "Constraint Dependent" function and therefore the population in each generation will be feasible for all chromosomes.

The "sampling mechanism" is assumed to be "linear ranking" and the "selection" (which is responsible for choosing the next productive generation for applying "mutation" or "crossover") is performed by "roulette wheel" using the probabilities calculated by "linear ranking mechanism".

To produce new generation (reproduction), "Elite Count" is assumed to be 2; this means that in "selection" process, two of best answers will always be selected for the next generation. The "Crossover Fraction" is assumed to be 0.8 initially; this leads to selecting of 80 % of the best answers for "crossover" and the remaining 20 % for "mutation" to make next generation. "Mutation Function" is considered as "constraint dependent" and "Crossover Function" as "Scattered" type. "Stopping Criteria" was chosen as:

1- The number of generation passes 100 and
2- The tolerance of "Fitness Function" becomes less than 10^{-6}

The initial values for GA parameters are the above mentioned values but during each round of simulation these values are updated until achieving the best results. Therefore due to different ground motions, for each optimization process the values of parameters are not the same as initial values.

These values are presented in Table 8. The optimization process has been done for seven design variables simultaneously for each of seven near-fault ground motions. Figure 10 shows the optimization process on the f_2 fitness function using GA algorithm. This figure shows the optimum values of seven design variables due to record No.4 according to Table 3. Figure 10a is a plot that shows the convergence of the mean and best values of each generation during reproduction. According to this figure the minimum obtained value of fitness function f_2 (Maximum Displacement in Isolation Level) is 251 mm.

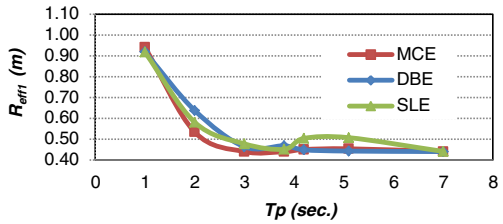

Fig. 12 Optimum values of R_{eff1} that minimize MDIL in three ground motion levels of MCE, DBE and SLE

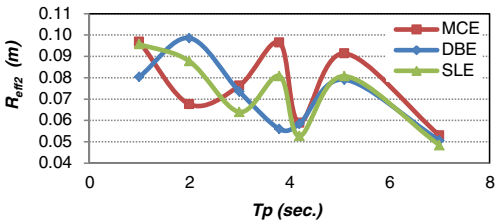

Fig. 14 Optimum values of R_{eff2} that minimize MRSD in three ground motion levels of MCE, DBE and SLE

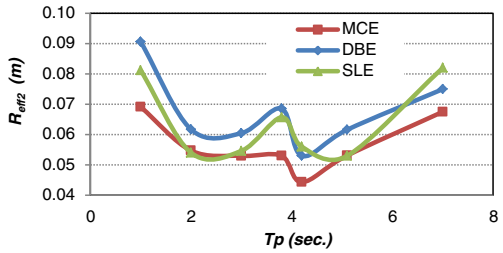

Fig. 15 Optimum values of R_{eff2} that minimize MDIL in three ground motion levels of MCE, DBE and SLE

7.2 Variation of optimum design variables

Optimum effective radius of sliding surfaces 1 and 4, R_{eff1} The results of optimization process for R_{eff1} that minimize the fitness function f_1 (MRSD) are plotted in Fig. 11 for three seismic hazard levels (MCE, DBE and SLE). As it is shown, the X axis displays the pulse period of the ground motion records according to Table 3. These pulse periods varies from 1 to 7 seconds. It can be concluded that for different hazard levels, the optimum values of R_{eff1} are in a close range and have a similar variation schema. The optimum values of R_{eff1} for wide range of pulse periods (between 1 and 6 seconds) are limited between 0.8 and 1 meter. Hence choosing a radius of curvature between 0.8 to 1 meter for sliding surface 1 and 4, the relative displacement of story will be minimized.

Figure 12 displays the optimum values of R_{eff1} that minimize fitness function f_2 (MDIL). As it is shown, for the periods less than 2.5 seconds, the optimum R_{eff1} are proportionally increased by reducing the pulse period. Moreover, it can be also concluded that the effect of ground motion level on optimum value of R_{eff1} is negligible. R_{eff1} has almost same optimum values for three SLE, DBE and MCE implicit levels. In this case the optimum values of R_{eff1} vary between 0.4 and 0.6 meter for a range of pulse period more than 2.5 seconds.

There is no obvious range for optimum values of R_{eff1} for minimizing function f according to Fig. 13, but it can be seen that the optimum values are so closed for different hazard levels. An interval between 0.7 and 1 meter can be recommended as optimum effective radius of sliding surfaces 1 and 4.

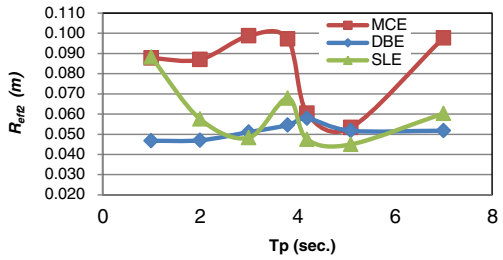

Fig. 16 The optimum values of R_{eff2} for combined objective function f in three levels of MCE, DBE and SLE

Optimum effective radius of sliding surfaces 2 and 3, R_{eff2} For effective radius of curvature of sliding surfaces 2 and 3, as it is shown in Fig. 14, there is no specific trend of variation for optimum values that minimize MRSD. According to this figure, the optimum values of R_{eff2} vary between 0.06 and 0.1 meter. For the ground motions with pulse periods greater than 4 seconds, it can be also concluded that the levels of hazards do not affect the optimum values.

Figure 15 shows the optimum values of R_{eff2} for fitness function f_2 (minimizing MDIL). The optimum values for three levels of hazard have a dished shape of variation. It can also be concluded that the displacement of isolator level will be minimum if R_{eff2} varies in a range between 0.05 and 0.07 meter.

For combined objective function f, as shown in Fig. 16, there is no definite optimum range for R_{eff2}.However for DBE hazard level it can be seen that the optimum values are confined in a range between 0.05 and 0.06 meter.

Coefficient of friction of sliding surface 1, μ_1 According to Fig. 17a, for coefficient of friction of sliding surface 1 with the variation interval between 0.06 and 0.018, no clear range of optimum values could be found that minimize fitness function f_1. Having a close look at Fig. 17a, for earthquake records with pulse periods smaller than 5 seconds, levels of hazard do not affect the optimum values of μ_1**.** The diagram of Fig. 17b shows the optimum values of μ_1 that minimize fitness function f_2. This diagram shows that for a wide range of pulse period of ground motions, the optimum values of μ_1 are so close to each other at different hazard levels. Due to convex shape of the diagram, the maximum optimum coefficients of frictions are obtained for records with approximate pulse periods of 4 second. For the earthquake records with pulse periods between 2 and 6 seconds, the optimum values vary in a range between 0.04 and 0.06.

To minimize combined objective function f, in MCE and DBE hazard levels and pulse period ranges between 1 to 6 seconds, the optimum values of μ_1 vary between 0.04 and 0.06 according to Fig. 17c, but for SLE hazard level, there is a high fluctuation and no range can be proposed.

Coefficients of friction of sliding surfaces 2 and 3, μ_2 The optimum values ofμ_2 to minimize fitness functions f_1 and f_2, are displayed in Fig. 17d and e. There is no specific routine in the shape of variation of optimum values, but due to less effect of μ_2 on the response of structure (especially

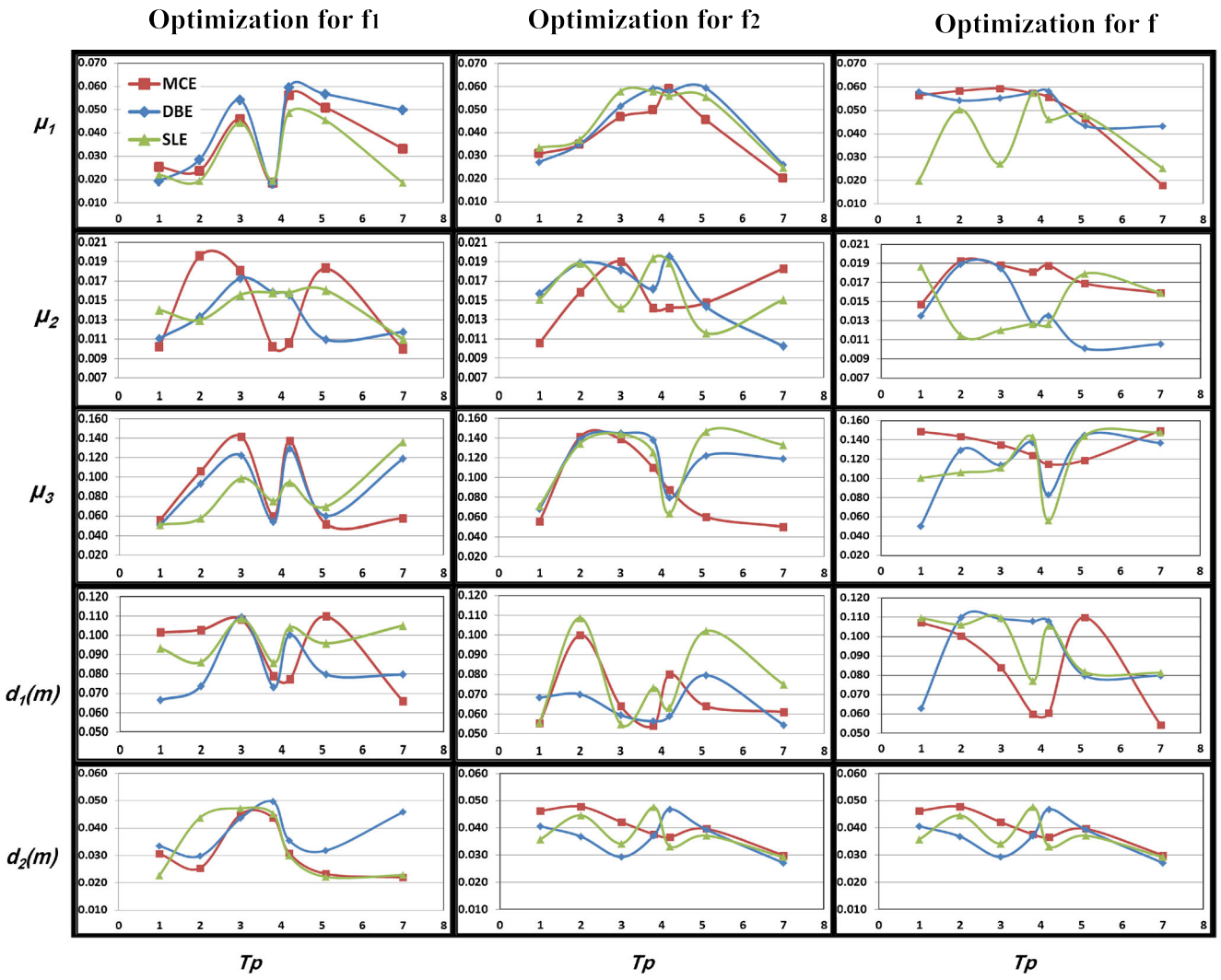

Fig. 17 Optimum values of TFPB variables (μ_1, μ_2, μ_3, d_1 *and* d_2) that minimize MRSD (f_1), MDIL (f_2) and combined objective function (f), in three ground motion levels of MCE, DBE and SLE

on displacement in isolator level), choosing optimum values will not be an important issue. This also can be seen in Fig. 17f that shows optimum values of $\mu_2$for $f$function.

Coefficient of friction of sliding surface 4, μ_3 Figure 17 g shows that the optimum values of μ_3 in different levels of hazard are very close when the fitness function is f_1. As it is shown, the optimum values of μ_3 have a sinusoidal

Table 9 Proposed range for design variables to minimize fitness functions f_1 and f_2 *and* Combined Objective function f

Design variable	Range for minimizing f_1(MRSD)	Range for minimizing f_2(MDIL)	Range for minimizing f(MRSD,MDIL)	Proposed optimum value
R_{eff1}(m)	0.8 – 1	0.4 – 0.6	0.7 – 1	06 – 0.8
R_{eff2}(m)	0.06 – 0.1	0.05 – 0.07	0.5 – 0.07	0.06
μ_1	0.02 – 0.06	0.04 – 0.06	0.045 – 0.06	0.05
μ_2	0.01 – 0.018	0.015 – 0.018	0.013 – 0.019	0.015
μ_3	0.06 – 0.14	0.08 – 0.14	0.1 – 0.15	0.1
d_1(m)	0.08 – 0.11	0.06 – 0.08	0.08 – 0.11	0.08
d_2(m)	0.02 – 0.035	0.04 – 0.05	0.03 – 0.05	0.035

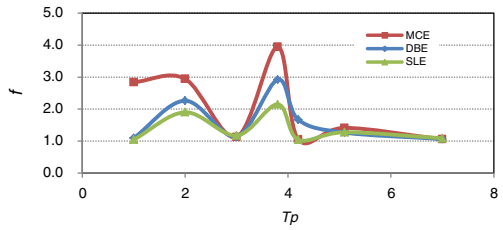

Fig. 18 The minimum values of combined objective function f due to optimum values of design variables in three hazard levels

shape for different pulse periods of ground motions. The optimums values of μ_3 for fitness function f_2 are plotted in Fig. 17h. It can be concluded from this figure that the optimum values of μ_3 are close in different hazard levels of ground motions with pulse periods between 1 and 4 seconds. For MCE hazard level, the maximum optimum values of μ_3 are obtained in the ground motions with a pulse period of 3 seconds. The optimum values of μ_3 for f function is plotted in Fig. 17i. The optimum values fluctuate between 0.1 and 0.14.

Displacement capacity of sliding surfaces 1 and 4, d_1 Figure 17j exhibits the optimum values of d_1 for fitness function f_1 in three levels of hazard. The optimum values vary between 0.08 and 0.11 meter. However the shape of optimum values in DBE and SLE levels are somehow similar but there is a considerable difference between the optimum values in different hazard levels. Considering Fig. 17k, the optimum values of d_1 that minimize the isolator level displacement vary between 0.06 and 0.08 meter. There is no specific schema in the variation of optimum values of d_1 in three levels of seismic hazards. The optimum values of d_1 for combined objective function f are plotted in Fig. 17l.

Displacement capacity of sliding surfaces 2 and 3, d_2 Figure 17m, n and o show the optimum values of d_2 that minimize fitness functions f_1, f_2 and f. Due to the small effect of d_2 on the response of structure, the error in choosing a range for optimum values will not significantly affect the minimum values of fitness functions. Hence a variation range between 0.03 and 0.05 meter will be reasonable.

7.3 Proposed ranges for the design variables to minimize fitness functions

According to the figures and comments in the last section, Table 9 proposes ranges of optimum values that minimize maximum relative story displacement (MRSD) and maximum story acceleration (MDIL). For more effective variables such as R_{eff1} and μ_1, choosing the value in the proposed ranges can significantly reduce the response of the structure; however for less important design variables such as μ_4 and d_2 these ranges are not so definite. In fact the optimum values of such variables are influenced by more effective ones due to satisfying the "fully adaptive" behavior of the TFPB.

Figure 18 shows the minimum values of function f in different hazard levels. As it is shown for some of ground motions the minimum value of f is close to one. According to the definition of function f, this means that both of single-objective functions f_1 and f_2 are at their minimum values. So the design variables can be arranged in a way that minimizes both of structural responses simultaneously. This shows the exclusive specification of TFPBs.

Table 9 also proposes a range of optimum values for design variables in its 4th column. These ranges are so operative for more effective design variables such as R_{eff1}, μ_1 and d_1. However these ranges are obtained due to an engineering judgment on the results of optimization process on combined objective function f.

At the 5th column of Table 9, an optimum range or value is proposed considering all of the optimum ranges for different fitness functions. These ranges and values can significantly control the response of the short to medium height structures.

8 Conclusion

The goal of this paper was to propose a method to design the variables of TFPBs used in isolated structures imposed by near-fault ground motions. In this process first the mechanical behavior of the TFPBs was modeled by three single FP elements in series and the variables of this series model were obtained based on TFPB design variables. The state equations for an isolated structure were derived parametrically and solved numerically using MATLAB considering the response history analysis. The obtained numerical solutions were verified by comparing to other published works. Next, the response of structure to fluctuations of design variables was evaluated by sensitivity analysis. Seven different records of near-fault ground motions with pulse periods between 1 and 7 seconds in three hazard levels were considered for analysis. Finally, Genetic Algorithm was applied to optimize the design variables for two single and one combined objective functions. Consequently, to minimize the structural responses, ranges of optimum values for design variables were proposed. The conclusions are summarized as following:

– Seven considered design variables do not exhibit the same effect on structural response in optimization process. For example the effective radius of curvature of sliding surfaces 1 and 4 has more important role in

changing the structural responses than the effective radius of curvature of sliding surfaces 2 and 3. This is the same for other variables such as coefficient of frictions and displacement capacities of different sliding surfaces, where the variables related to sliding surfaces 2 and 3 have much less effect on the values of maximum structural responses.

- Except some cases the optimum design variables were closed to each other in three levels of MCE, DBE and SLE and therefore the influence of hazard levels is negligible and the particular hazard levels which were selected in this study does not limit the generality of the obtained results for optimum parameters.
- For variables such as effective radius of curvatures of surfaces 1 and 4, a close range is proposed for optimum values. However this range is not the same for minimizing different structural responses.
- For some ground motions, the obtained minimum values for combined objective function "f" shows that the maximum responses of structure can simultaneously take their minimum values.
- An optimum range or values were proposed considering all of the optimum ranges for different fitness functions.
- Due to the fact that the base isolation systems are mostly designed for low and medium height buildings and the serving superstructures have a rigid dynamic behavior, and also considering the fact that the mass of superstructures does not affect the vibration periods of structures isolated via friction pendulum bearings (unlike the ones isolated with elastomeric isolators), the results of optimization process in this research can be further applied for different structures.

References

Alavi B, Krawinkler H (2001) Effects of near-fault ground motions on frame structures. John A. Blume Earthquake Engineering Center

Baker JW (2007) Quantitative classification of near-fault ground motions using wavelet analysis. Bull Seismol Soc Am 97(5):1486–1501

Bertero VV, Mahin SA, Herrera RA (1978) Aseismic design implications of near fault san fernando earthquake records. Earthq Eng Struct Dyn 6(1):31–42

Constantinou M, Mokha A, Reinhorn A (1990) Teflon bearings in base isolation II: modeling. J Struct Eng 116(2):455–474

Fenz DM (2008) Development, Implementation and Verification of Dynamic Analysis Models for Multi-spherical Sliding Bearings. ProQuest

Fenz DM, Constantinou MC (2008a) Mechanical behavior of multi-spherical sliding bearings. vol 7. Multidisciplinary Center for Earthquake Engineering Research

Fenz DM, Constantinou MC (2008b) Modeling triple friction pendulum bearings for response-history analysis. Earthq Spectra 24(4):1011–1028

Fenz DM, Constantinou MC (2008c) Spherical sliding isolation bearings with adaptive behavior: theory. Earthq Eng Struct Dyn 37(2):163–183

Goldberg DE (1989) Genetic algorithm in search. Optim Mach Learn

Hall JF, Heaton TH, Halling MW, Wald DJ (1995) Near-source ground motion and its effects on flexible buildings. Earthq Spectra 11(4):569–605

Jangid R (2005) Optimum friction pendulum system for near-fault motions. Eng Struct 27(3):349–359

Kelly JM, Naeim F (1999) Design of seismic isolated structures: from theory to practice. Wiley, Nueva York

Malekzadeh M, Taghikhany T (2012) Multi-stage performance of seismically isolated bridge using triple pendulum bearings. Adv Struct Eng 15(7):1181–1196

Mayes RL, Naeim F (2001) Design of structures with seismic isolation. In: The seismic design handbook. Springer, pp 723–755

Michalewicz Z (1995) A survey of constraint handling techniques in evolutionary computation methods. Evol Program 4:135–155

Moeindarbari H, Malekzadeh M, Taghikhany T (2014) Probabilistic analysis of seismically isolated elevated liquid storage tank using multi-phase friction bearing. Earthq Struct 6(1):111–125. doi:10.12989/eas.2014.6.1.111

Mokha A, Constantinou M, Reinhorn A (1990) Teflon bearings in base isolation I: testing. J Struct Eng 116(2):438–454

Tsai C, Chen B-J, Pong W, Chiang T-C (2004) Interactive behavior of structures with multiple friction pendulum isolation system and unbounded foundations. Adv Struct Eng 7(6):539–551

Yang Y, Lu L, Yau J (2005) Chapter 22: structure and equipment isolation. Vibration and Shock Handbook

Zayas VA, Low SS, Mahin SA (1990) A simple pendulum technique for achieving seismic isolation. Earthq Spectra 6(2):317–333